The Influence of a Mainstream Thermal Boundary Layer on Film Effectiveness

D. E. Paxson

R. E. Mayle

Department of Mechanical Engineering,
Rensselaer Polytechnic Institute,
Troy, NY 12181

A theoretical and experimental investigation on the effect of a mainstream thermal boundary layer on adiabatic film effectiveness is presented. The theory is based on a simple model which accounts for mixing between the injected flow and a mainstream flow with a viscous and thermal boundary layer. In order to apply this theory, the adiabatic film effectiveness in a flow with uniform temperature must be known either from experiments or from another theory. Experiments are described for an injection geometry having a simple two-dimensional slot. These tests were conducted with an insulated lip having a lip-diameter to slot-height ratio of 0.6. The mainstream thermal boundary layer was produced by heating the surface in contact with the mainstream flow upstream of the slot. Velocity and temperature distributions were measured at various distances downstream of the slot, along with measurements of the adiabatic wall temperatures. All tests were performed at a secondary to mainstream mass flux ratio of 0.7, but with different amounts of mainstream heating. While a comparison between theoretical and experimental results shows a discrepancy near injection, the trend is correct, and the agreement downstream is good.

Introduction

Within the last twenty years, film cooling has become a common method of protecting mechanical components from hot gaseous environments. Examples abound in modern gas turbine engines, as described by Metzger and Mayle (1983), where combustor linings and components in the first two stages of the turbine are usually film cooled. In many cases, film cooling is combined with conventional convective cooling methods so that the air, after passing through the cooling channels, is used for film cooling.

Usually, heat transfer with film cooling is determined by using a film heat transfer coefficient h_f and an adiabatic wall or film temperature T_{aw} as described by Goldstein (1971), i.e.,

$$q_f = h_f(T_{aw} - T_w)$$

where T_w is the component wall temperature. Introducing the adiabatic wall or film effectiveness η defined as

$$\eta = \frac{T_\infty - T_{aw}}{T_\infty - T_s}$$

where T_∞ and T_s are the mainstream and secondary or injected air temperatures, respectively, the surface heat flux with film cooling is obtained from

$$q_f = h_f(T_\infty - T_w)\left[1 - \eta\left[\frac{T_\infty - T_s}{T_\infty - T_w}\right]\right]$$

Both h_f and η must be known before the heat flux can be obtained and both depend, at least, on the injection geometry, coolant-to-mainstream mass and momentum flux ratios, and the distance measured from injection. They are usually obtained experimentally and, in the past, most effort has been spent in measuring the film effectiveness η. Effectiveness experiments are conducted under nearly adiabatic conditions where the mainstream air temperature is uniform.

Difficulties do not usually arise in using the adiabatic effectiveness determined in this manner unless coolant is used to cool the surface preceding injection, injection is preceded by another film injection, or simply stated, the mainstream thermal boundary layer is thick compared to the "equivalent slot height" of the injection scheme. In this case, the mainstream temperature profile at injection does not resemble that under which the effectiveness measurements were obtained, namely, constant and equal to T_∞. As a result, when the measured effectiveness distribution is used together with the perceived mainstream temperature, the heat flux is overestimated.

Sellers (1963) was first to make this point and proposed a method to account for the case of multiple film injections. The method is simple in that the mainstream temperature is replaced by the local adiabatic wall temperature, which results from all preceding injections. In order to predict the correct result, the method requires that the temperature profiles should be relatively flat near the wall and up to the height of injection. Its simplicity however, has made it a mainstay in design systems for multiple film injections.

Contributed by the International Gas Turbine Division and presented at the 33rd International Gas Turbine and Aeroengine Congress and Exhibition, Amsterdam, The Netherlands, June 5-9, 1988. Manuscript received by the International Gas Turbine Division September 15, 1987. Paper No. 88-GT-17.

Situations without previous film injections, but with a significant thermal deficit in the mainstream boundary layer, remain to be analyzed. It is this problem that the present paper addresses.

Theory

Consider the control volume shown in Fig. 1. Consider the upper boundary of the control volume to be a streamline and assume that, for any such control volume that can be drawn downstream of the slot, the fluid from the slot has completely mixed with the mainstream fluid up to the height y as shown. If the specific heats of the fluids are considered identical and constant, an energy balance can be written in the following form:

$$\int_0^y \rho_\infty u_\infty T dy + \rho_s U_s T_s s = T_{aw}\left[\int_0^y \rho_\infty u_\infty dy + \rho_s U_s s\right]$$

where the subscripts ∞ and s refer to the mainstream and secondary fluid, respectively, $u_\infty = u_\infty(y)$ is the streamwise velocity, U_s is the average velocity in the slot, T is the temperature, s is the slot height, and T_{aw} is the adiabatic wall temperature. In addition to the above assumptions, it has also been assumed that the conduction of heat across the upper streamline boundary of the control volume can be neglected compared to the slot energy deficit $\rho_s U_s c(T_\infty - T_s)s$, where c is the specific heat. Thus, the theoretical model simply considers the downstream increase in the adiabatic wall temperature to be the result of a progressively upward mixing of the slot fluid with a hotter mainstream fluid. As such, y, the distance up to which mixing has occurred, and T_{aw} are intimately connected, as will be shown later. Although a flat, completely mixed-out temperature profile has been assumed at the downstream boundary of the control volume, it is only necessary to assume that the profiles for every such control volume are similar (such as done by Wieghardt, 1964) and that the mixing occurs as previously described. For these more realistic conditions, the results will be identical to those presented below. The above expression may be rearranged to yield

$$\eta = \frac{T_\infty - T_{aw}}{T_\infty - T_s} = \frac{\int_0^y \frac{u_\infty}{U_\infty}\left[\frac{T_\infty - T}{T_\infty - T_s}\right]dy + Ms}{\int_0^y \frac{u_\infty}{U_\infty}dy + Ms}$$

where the mainstream velocity U_∞ and the coolant mass flux ratio $M = \rho_s U_s / \rho_\infty U_\infty$ have been introduced.

For the case where no thermal deficit in the mainstream exists, one has $T = T_\infty$ everywhere in the mainstream, and the integral in the numerator is zero. Therefore, the adiabatic film effectiveness, η_a is given as

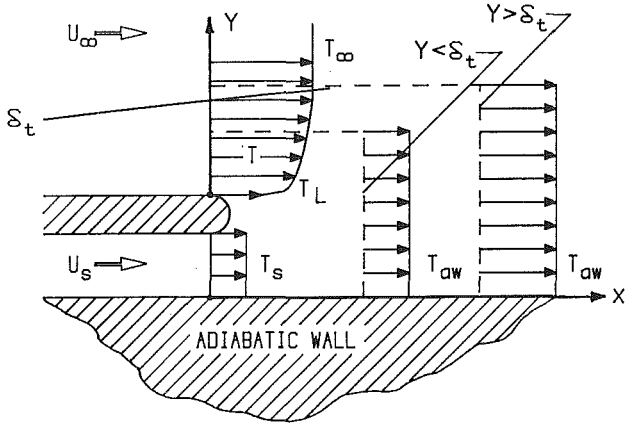

Fig. 1 Control volumes for energy balance with $y \le \delta_t$ and $y \ge \delta_t$

$$\eta_a = Ms\left[\int_0^y \frac{u_\infty}{U_\infty}dy + Ms\right]^{-1} \quad (1)$$

This expression is identical to that obtained by Goldstein (1971). Substituting this into the original effectiveness equation provides

$$\eta = \eta_a\left\{\frac{1}{Ms}\int_0^y \frac{u_\infty}{U_\infty}\left[\frac{T_\infty - T}{T_\infty - T_s}\right]dy + 1\right\}$$

A lip effectiveness ϕ may be defined as

$$\phi = \frac{T_\infty - T_L}{T_\infty - T_s}$$

where T_L is the lip temperature on the surface adjacent to the mainstream. The above expression then becomes

$$\eta = \eta_a\left\{\frac{\phi}{Ms}\int_0^y \frac{u_\infty}{U_\infty}\left[1 - \frac{T - T_L}{T_\infty - T_L}\right]dy + 1\right\} \quad (2)$$

This expression can only be evaluated if the mainstream velocity and temperature distributions at the slot, i.e., $x = 0$, and the streamwise distribution of the adiabatic film effectiveness, η_a, are known. In what follows, it will be presumed that η_a is known from either experiment or another theory. In order to assess the effect of a mainstream thermal boundary layer, it will be assumed that both the mainstream velocity and temperature profiles at the lip obey a simple power law approximation, i.e.,

$$\frac{u_\infty}{U_\infty} = \left[\frac{y}{\delta}\right]^{\frac{1}{n}} \equiv \gamma^{\frac{1}{n}} \text{ and } \frac{T - T_L}{T_\infty - T_L} = \left[\frac{y}{\delta_t}\right]^{\frac{1}{n}} = (\gamma/r)^{\frac{1}{n}}$$

where r is the ratio of the thermal to viscous bounday layer thickness, $r = \delta_t/\delta$.

Substituting the above expression for the velocity profile into equation (1), integrating, and rearranging, one obtains

Nomenclature

c = specific heat
h_f = heat transfer coefficient with film cooling
M = secondary-to-mainstream mass flux ratio
q_f = surface heat flux with film cooling
r = Thermal to viscous boundary layer thickness
s = slot height
T = temperature
u = local streamwise velocity = $u(y)$
U = free-stream or average velocity
x = streamwise distance measured from slot exit
y = distance measured normal from upper lip surface
y_1 = distance measured normal from adiabatic surface
γ = dimensionless distance normal to upper lip surface
δ_1 = displacement thickness
δ_2 = momentum thickness
Δ_2 = enthalpy thickness
η = adiabatic film effectiveness
η_a = adiabatic film effectiveness without heated lip surface
ρ = density
ϕ = dimensionless lip temperature

Subscripts

aw = adiabatic wall
L = Lip
s = secondary air
w = wall
∞ = mainstream air

$$\gamma = \left\{ \left[\frac{\delta}{Ms} \right]^{-1} \left[\frac{n+1}{n} \right] \left[\frac{1-\eta_a}{\eta_a} \right] \right\}^{\frac{n}{n+1}} \tag{3}$$

This may now be regarded as the height in the mainstream flow above the lip to which mixing occurs for a control volume that extends to $x = x(\eta_a)$, i.e., this expression relates the height of any one control volume to its length. Note that in the following any single control volume is not changing, but that numerous control volumes are being considered.

There are now at least two cases to evaluate: that for $\gamma \le r$ and that for $\gamma \ge r$. The first is for all control volumes where the mixing height y is less than the thermal boundary layer thickness δ_t. This generally corresponds to small distances from injection, say $0 \le x \le x_r$. The second case is that where mixing has occurred beyond the thermal boundary layer, into the region where the mainstream temperature is constant. It corresponds to large distances from injection, $x \ge x_r$. In addition, one may have either $r \le 1$ or $r \ge 1$. Substituting the assumed form for the velocity and temperatures profiles into equation (2) and integrating yields

$$\frac{\eta}{\eta_a} = 1 + \phi \left(\frac{\delta}{Ms} \right) \left[\frac{n}{n+1} \gamma^{\frac{n+1}{n}} - \frac{n}{n+2} r^{-\frac{1}{n}} \gamma^{\frac{n+2}{n}} \right]$$

which upon substituting into equation (3) provides

$$\frac{\eta}{\eta_a} = 1 + \phi \frac{1-\eta_a}{\eta_a} \left\{ 1 - \frac{n+1}{n+2} r^{-\frac{1}{n}} \left[\frac{n+1}{n} \frac{Ms}{\delta} \frac{1-\eta_a}{\eta a} \right]^{\frac{1}{n+1}} \right\} \tag{4}$$

This expression implicitly relates the film effectiveness with a mainstream thermal deficit, η, to the streamwise distance x through the functional $\eta_a = \eta_a(x)$, which in turn has been assumed known. The restriction $\gamma \le r \le 1$ requires (see equation (1))

$$\eta_a \ge \left[1 + \frac{n}{n+1} \frac{\delta}{Ms} r^{\frac{n+1}{n}} \right]^{-1} \ge \left[1 + \frac{n}{n+1} \frac{\delta}{Ms} \right]^{-1}$$

In other words, equation (4) is valid for the region between the slot ($x = 0$) and the distance $x = x_r$, which corresponds to the position where η_a equals the first expression in the above restriction. Beyond this point η continues to decrease as mixing continues. In this region, however, mixing occurs with air at the free-stream temperature T_∞. Thus, the integrand in equation (2) is zero for $y \ge \delta_t$ or $x \le x_r$. The upper limit to the integral becomes $\gamma = r$ and one obtains

$$\frac{\eta}{\eta_a} = 1 + \frac{n}{(n+1)(n+2)} \phi \left(\frac{\delta}{Ms} \right) r^{\frac{n+1}{n}}; \quad (x \ge x_r) \tag{5}$$

This result is valid for $\gamma \ge r$ ($y \ge \delta_t$) provided that $r \le 1$ ($\delta_t \le \delta$) and implies that beyond $x = x_r$, the film effectiveness with a thermal boundary layer is a simple multiple of that without. This completes the necessary analysis for all of the cases corresponding to $r \le 1$.

The cases corresponding to $r \ge 1$ are as easily determined as those above, but result in somewhat more complicated expressions. Integration of equation (2) with the assumed velocity and temperature profiles, noting that $u_\infty = U_\infty$ for $y \ge \delta$ yields

$$\frac{\eta}{\eta_a} = 1 + \phi \frac{1-\eta_a}{\eta_a} \left\{ 1 - \frac{n+1}{n+2} r^{-\frac{1}{n}} \left[\frac{n+1}{n} \frac{Ms}{\delta} \frac{1-\eta_a}{\eta_a} \right]^{\frac{1}{n+1}} \right\}$$

for

$$\eta_a \ge \left[1 + \frac{n}{n+1} \frac{\delta}{Ms} \right]^{-1}$$

which is identical to equation (4) and corresponds to $y \le \delta$.

$$\frac{\eta}{\eta_a} = 1 + \phi \left\{ \frac{1-\eta_a}{\eta_a} - \frac{n}{n+1} \frac{\delta}{Ms} r^{-\frac{1}{n}} \left[\left[\frac{1}{n+1} + \frac{Ms}{\delta} \frac{1-\eta_a}{\eta_a} \right]^{\frac{n+1}{n}} - \frac{1}{n+2} \right] \right\} \tag{6}$$

for

$$\left[1 + \frac{\delta}{Ms} \left[r - \frac{1}{n+1} \right] \right]^{-1} \le \eta_a \le \left[1 + \frac{n}{n+1} \frac{\delta}{Ms} \right]^{-1}$$

which corresponds to $\delta \le y \le \delta_t$, and finally

$$\frac{\eta}{\eta_a} = 1 + \phi \frac{\delta}{Ms} \left[\frac{r-1}{n+1} + \frac{n}{(n+1)(n+2)} r^{-\frac{1}{n}} \right] \tag{7}$$

which corresponds to $y \ge \delta_t$.

All of the above equations show that there are four parameters on which the actual, or corrected, effectiveness depends. The first is the ratio of thermal to viscous boundary layer thicknesses, $r = \delta_t/\delta$; the second is the mainstream boundary layer to secondary mass flow ratio, δ/Ms; the third is the dimensionless lip temperature ϕ; and the last is the power of the assumed velocity and temperature profiles, $1/n$. From either equation (4) or (5) it is obvious that $(\eta/\eta_a) - 1$ is directly proportional to the dimensionless lip temperature ϕ, which suggests plotting the theory in the form $1/\phi\ (\eta/\eta_a - 1)$ versus η_a. Such a plot is shown in Fig. 2, where the values for r, δ/Ms, and n are 0.9, 2, and 7, respectively. These values are similar to those for the present experiment. A decrease in the abscissa (decreasing η_a) corresponds to an increase in the distance from the slot. The regions corresponding to $x \ge x_r$ and $x \le x_r$ are marked in the figure. For typical gas turbine conditions $\phi \cong 0.75$. Thus the maximum gain in film effectiveness resulting from a mainstream thermal boundary layer having the conditions used in Fig. 2 would be about 12 percent. Maximum gains for other conditions can be readily obtained from either equation (5) or (7). A maximum gain of about 20 percent is predicted from the more realistic ratio of thermal to viscous boundary layer thicknesses, $r = 1.4$.

Experimental Facility

The tests were performed using a low-speed test facility with separate mainstream and secondary air supply systems. The mainstream air supply system was an open-circuit wind tunnel powered by a centrifugal fan. A plenum containing baffles and screens followed by a nozzle insured a uniform mainstream flow in the test section. Thermocouples located upstream of the nozzle were used to measure the mainstream air temperature. The mainstream flow velocity was measured

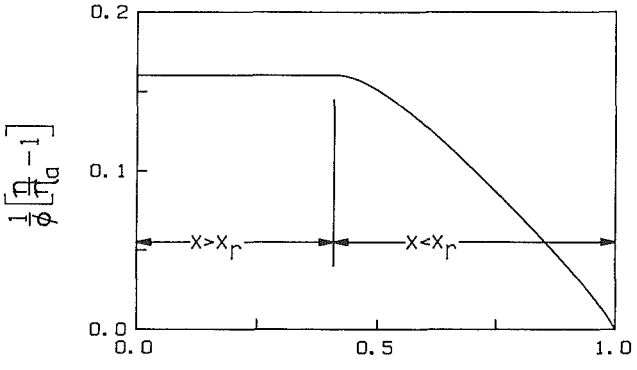

Fig. 2 Theoretical result for $r = 0.9$, $\delta/Ms = 2$, and $n = 7$

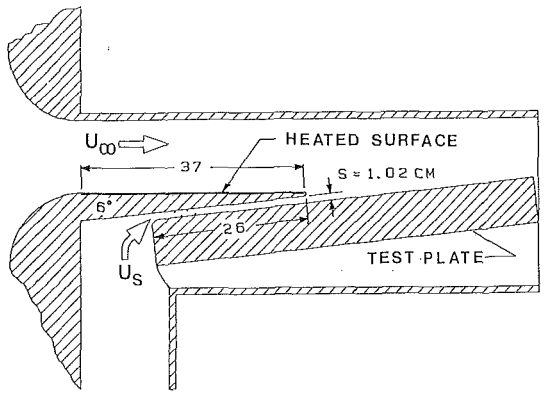

Fig. 3 Test section with slot injection and a lip with a heated surface

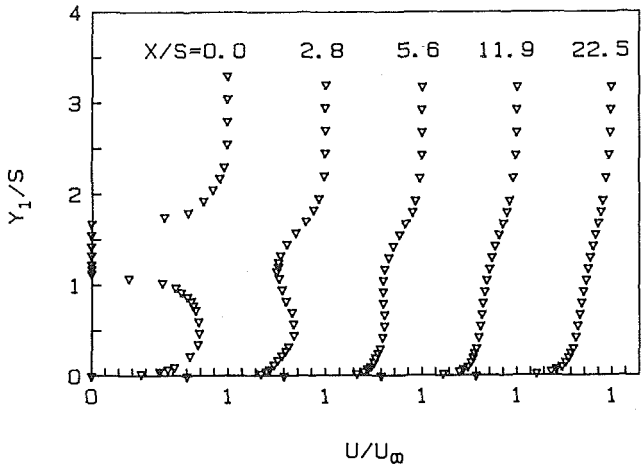

Fig. 4 Velocity profiles at different downstream positions, $M = 0.7$

using a Kiel probe, and a static pressure tap located within the test section. The secondary air supply consisted of a centrifugal fan, a heating chamber, and a secondary air plenum chamber. The latter was directly attached to the test section. The heating chamber contained four individually regulated heating units of stranded nichrome wire sandwiched between sets of filtering screens. The plenum contained a series of screens and baffles, which provided a uniform injection flow. The secondary mass flow rate was obtained using a calibrated nozzle positioned between the heating and plenum chambers. The secondary air temperature was measured directly at the slot exit.

The test section is shown in Fig. 3. It was composed of a top wall, a heated-lip model, and an "adiabatic" test plate attached to plexiglass sidewalls. The width of the test section was 30.5 cm and its height before the slot was 12.7 cm. Four trip wires were mounted at the slot entrance to insure turbulent flow within the channel. The heated-lip model is 37 cm long and had a lip diameter of 0.64 cm. The model was designed to provide an injection angle of 6 deg and was positioned to provide a slot height of $s = 1.02$ cm. The model was made primarily from plywood and balsa wood. The upper surface of the model (that in contact with the mainstream flow) was covered with a heating unit, which consisted of a continuous 2.54-cm steel foil strip folded back and forth to create a "heating sheet". The foil was sandwiched between two layers of fiberglass, bonded to the upper surface of the model, and connected to an a-c power supply. Thermocouples positioned at various locations throughout the model were used to measure the upper and lower lip surface temperatures. The entire model was painted with a flat black enamel finish that had an emissivity of 0.985.

The test plate was 30.5 cm wide and 64 cm long. It was constructed from a 1.27-cm-thick plywood support plate covered with a 2.54-cm-thick balsa wood layer. This arrangement provided a nearly adiabatic wall for measuring film effectiveness. Seventeen thermocouples, mounted in the surface from $x/s = -3.75$ to 36.25 along the center of the plate, were used to obtain the adiabatic surface temperatures. Thermocouples located to either side of center were used to check the two dimensionality of the flow. In addition, thermocouples located on the back of the test plate were used to evaluate the conduction losses through the test plate. In order to further reduce back loss, the space behind the test plate was filled with fiberglass insulation. All of the thermocouples were connected to junction blocks located within the test plate. As with the model, the entire test plate was coated with flat black enamel.

All tests were conducted with the mainstream air velocity and temperature nominally maintained at 18.3 m/s and 19°C, respectively. The mass flux ratio was maintained at a constant nominal value of $M = 0.7$. The secondary air and lip temperatures depended on the value of ϕ and varied between $30 \le T_S \le 50$°C and $25 \le T_L \le 50$°C, respectively. It should be noted that with a heated secondary flow, $T_S \ge T_\infty$, and no surface heating, the lip temperature was always somewhat greater than the mainstream air temperature, i.e., $\phi \ge 0$, because of conduction through the lip.

The velocity and temperature profile measurements were obtained using a vertical traversing mechanism, which could be moved in the streamwise direction to various x/s positions. Velocity traverses were performed using a miniature boundary layer total pressure probe. These traverses were taken with the mainstream and secondary air at the same temperature. For each x/s position traversed, a static pressure tap was mounted in the sidewall at the same x/s location. Temperature traverses were made using a small thermocouple probe with flow conditions matching the effectiveness tests. The temperature traverses performed with the lip surface heated were conducted with the lip temperature equal to the secondary air temperature, i.e., $\phi = 1.0$.

The effectiveness tests were performed with the lip surface heated and unheated. The secondary air and lip surface temperatures (ϕ) were selected and the plenum and model heaters set appropriately. When all the mainstream and secondary flow rates and temperatures were set, the facility was run for a minimum of six hours in order to achieve a steady-state condition. At the end of this period, temperature readings from all of the thermocouples were recorded and the flow rates checked.

The effectiveness measurements were corrected for heat transfer losses by conduction through the test plate and radiation to the surroundings. A one-dimensional model of each surface element was used and a heat balance performed to obtain the "adiabatic" wall temperature. Radiation corrections were particularly difficult to ascertain exactly because the test surface radiates to the inside of the slot, as well as to the surrounding surfaces. However, corrections to the measured adiabatic film effectiveness due to radiation were always less than 7 percent and those due to conduction were less than 4 percent.

Results

Velocity and Temperature Profiles. The measured velocity profiles at several x/s positions are shown in Fig. 4, where the origin of each profile is shifted by 0.7 along the abscissa. In order to avoid confusion, the vertical distance y_1 is measured from the test surface, and not from the top of the lip as in the theory, i.e., $y_1 = y + s +$ lip thickness. The profile at the slot exit is seen to have a region directly behind the lip where the velocity is zero. The actual data gathered in this vicinity,

Table 1

x/s	δ_1/s	δ_2/s	H
0	1.07	0.30	3.57
2.8	0.53	0.37	1.43
5.6	0.49	0.36	1.36
11.9	0.45	0.34	1.32
22.5	0.43	0.33	1.30

however, registered a small negative pressure difference between total and static pressures. Because it was not certain whether this was caused by a slight difference between the mainstream and secondary static pressure, and because the readings were very small (within the error range of the manometer), the values were simply taken to be zero. The remaining profiles illustrate the mixing trend as the flow moves downstream. The final profile at $x/s=22.5$ looks very much like a typical flat plate turbulent profile. Values of the displacement thickness, momentum thickness, and shape factor are provided in Table 1. The shape factor for $x/s=22.5$ agrees well with the generally accepted value for a fully turbulent profile.

The temperature profiles for an unheated and a heated lip surface, $\phi=0.34$ and 1.07, respectively, are shown in Fig. 5. As with the velocity, these profiles are plotted as functions of y_1/s, but each profile is shifted along the abscissa by 0.8. The triangular symbol for each profile at $y_1/s=0$ represents the wall temperature measured by the thermocouples embedded in the wall, as opposed to the probe thermocouple. (Actually, the traverses were done at x/s positions that fell between wall thermocouples; thus an interpolation was performed.) In all traverses, this value was lower than the temperature measured by the probe. The discrepancy illustrates the effects of back loss through, and radiation from, the test surface. It is also due, in part, to conduction along the probe stem. Both sets of profiles exhibit behavior that is intuitively expected. At $x/s=0$ the profiles appear reasonably uniform up to the slot height. Above this there is a region that seems nearly linear. Here, in the wake of the lip, conduction appears to be the important heat transfer mechanism. Finally, a typical heated boundary layer profile is seen above the lip. Comparison of the profiles at $x/s=0$ shows for the heated case that a substantial amont of heat is contained both in the flow above the lip and in the wake. The latter is presumably a result of the downstream mixing and reverse flow in the wake. Moving downstream, mixing occurs and the additional thermal energy introduced by the heated surface becomes more and more diffuse.

The enthalpy thickness was evaluated for each traverse position for both the heated and unheated cases. The average value of Δ_2/s for the unheated case is 0.72, with a deviation from the mean of less than 10 percent. For the heated case, the value is $\Delta_2/s=0.79$, also with a deviation of less than 10 percent. Thus it appears as if the test facility represents a reasonably closed control volume. If the lip were truly adiabatic, it should be observed that the value of Δ_2/s would be equal to the mass flux ratio M. Recalling that a nominal value for M of 0.7 was used for the traverses, the above experimental result for the unheated surface, $\Delta_2/s=0.72$, is further reassurance for the accuracy of the data.

Effectiveness Results. The measured film effectiveness distributions for four different values of $\phi>0$ are plotted in Fig. 6 as functions of x/s. Here, as in the theory, η denotes the adiabatic film effectiveness with a mainstream thermal boundary layer. The data for $\phi=0.34$ were actually obtained without applying current to the heater strip on the lip surface and is simply a result of heat transferred from the secondary air by conduction through the lip.

Figure 6 indicates a rather significant effect caused by the presence of a mainstream thermal boundary layer. All of the

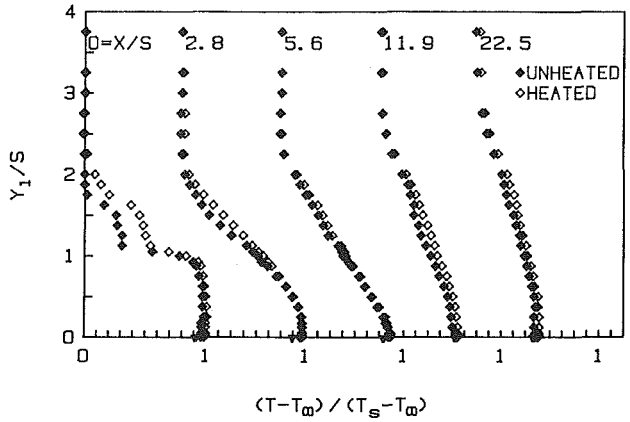

Fig. 5 Temperature profiles with and without lip surface heating

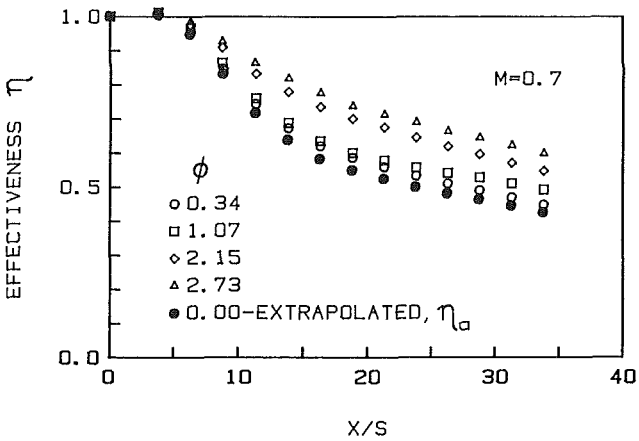

Fig. 6 Effectiveness results for different lip surface temperatures

effectiveness distributions follow the same trend, for a given value of ϕ. Each begins at the exit with $\eta=1$, and maintains nearly this value to about $x/s=6$. The effectiveness then drops off rapidly as mixing near the wall begins. Farther downstream the decay becomes more gradual. The effect of the lip boundary layer is seen as soon as the mixing near the wall begins. However, it is much more noticeable downstream after most of the mixing has occurred. Furthermore, it is seen that for a given x/s position, the effectiveness value increases with ϕ. A plot of η against ϕ for each streamwise position produces a linear correlation. This should be expected since the energy equation is linear and the heated case can be considered as the superposition of two thermal profiles, one of which has a constant mainstream temperature. In heat transfer tests, a constant mainstream temperature profile is impossible to achieve. Nevertheless, the truly adiabatic film effectiveness η_a can be obtained from these tests by a linear extrapolation of η versus ϕ to $\phi=0$ for each x/s position. This result is also presented in Fig. 6 and is denoted by the closed symbols as $\phi=0$-extrapolated, or simply η_a.

In Fig. 7, the film effectiveness η for two test conditions are plotted. In this figure, however, the results are plotted in the format suggested by the theory (Fig. 2). The solid symbols represent the average of the data previously plotted in Fig. 6 for the two highest values of ϕ. For this case, $\delta/Ms=1.96$. The second set of data was obtained for a thickened mainstream boundary layer having $\delta/Ms=2.65$ with $\phi=2.04$ and 2.78. In both cases, $\delta_t/\delta=0.76$. In addition, the theoretical results obtained from equations (4) and (5) are also shown.

In general, the overall trend at lower values of η_a (larger x/s), and the effects of boundary layer thickness, are reasonably well predicted. A major discrepancy between

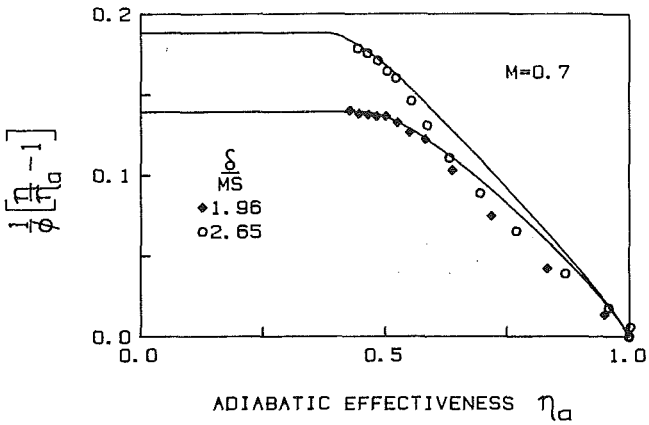

Fig. 7 Comparison of experimental results with theory, $M = 0.7$

theory and experiment, however, is noted at the higher values of η_a (smaller x/s). Theory consistently predicts a higher corrected effectiveness η than actually exists. The reason for this is presently attributed to the mixing process immediately downstream of injection. While the theory assumes mixing across the whole profile, the profile results indicate that the mixing occurs away from the lip until the wall is encountered. One may question why, contrary to the conventional notion, a higher degree of mixing would yield a higher effectiveness. The answer lies in the failure of conventional thinking to consider the effects of a mainstream boundary layer with an energy deficit. In this case, mixing more fluid with less energy improves the effectiveness. In light of the present results, then, it appears that the beneficial effect of the mainstream thermal boundary layer is not immediately realized to the extent predicted by the theory. As the mixing becomes more complete, however, the effect is more fully realized and the experimental and theoretical results compare quite favorably.

Conclusions

It is apparent that the adiabatic wall effectiveness is significantly altered by the presence of a thermal boundary layer in the mainstream flow. Since, in an actual turbine blade, this boundary layer always exists, one might question the accuracy of previous analyses, which assume the conventional adiabatic condition. In this respect, the effect studied here helps the designer.

It also appears that the simple theoretical model presented herein is quite adequate for estimating the effect of a mainstream thermal boundary layer on the film effectiveness. The model does, however require that the adiabatic wall effectiveness without a thermal boundary layer, η_a, be known a priori. In addition, one must also know the ratio of the mainstream thermal to viscous boundary layer thicknesses, δ_t/δ, and the ratio of the mass flow in the mainstream boundary layer to that injected, δ/Ms. Since η_a itself is used as a measure of the mixing that actually takes place, it appears that the model may be applied to injection geometries other than the slot.

Acknowledgments

The theory was developed while the second author was visiting the Institut für Thermische Strömungsmaschinen, Universität Karlsruhe, Karlsruhe, Federal Republic of Germany, under the Sonderforschungsbereich 167, Jan. 1985.

References

Goldstein, R. J., 1971, "Film Cooling," *Advances in Heat Transfer*, Academic Press, Vol. 7, pp. 321–379.

Metzger, D. E., and Mayle, R. E., 1983, "Gas Turbine Heat Transfer," *Mechanical Engineering Magazine*, Vol. 105, 6, pp. 44–52.

Seller, J. P., 1963, "Gaseous Film Cooling With Multiple Injection Stations," *AIAA Jour.*, Vol. 1, 9, pp. 2154–2156.

Wieghardt, K., 1946, "Hot-Air Discharge for De-Icing," AAF Translation No. F-TS919-RE, Air Material Command.